# Improved control of a prosthetic limb by surgically creating electro-neuromuscular constructs with implanted electrodes

Jan Zbinden[1,2], Paolo Sassu[1,3,4], Enzo Mastinu[1,2,5], Eric J. Earley[1,2], Maria Munoz-Novoa[1,6], Rickard Brånemark[7,8,9], Max Ortiz-Catalan[1,2,10*]

[1] Center for Bionics and Pain Research, Mölndal, Sweden.
[2] Department of Electrical Engineering, Chalmers University of Technology, Gothenburg, Sweden.
[3] Department of Hand Surgery, Sahlgrenska University Hospital, Mölndal, Sweden.
[4] Department of Orthoplastic, IRCCS Istituto Ortopedico Rizzoli, Bologna, Italy.
[5] The BioRobotics Institue, Scuola Superiore Sant'Anna, Pisa, Italy.
[6] Center for Advanced Reconstruction of Extremities, Sahlgrenska University Hospital, Mölndal, Sweden.
[7] Center for Extreme Bionics, Biomechatronics Group, MIT Media Lab, Massachusetts Institute of Technology, Cambridge, USA.
[8] Department of Orthopaedics, Gothenburg University, Gothenburg, Sweden.
[9] Integrum AB, Mölndal, Sweden
[10] Bionics Institute, Melbourne, Australia.



The definitive version was published in:
Science Translational Medicine
Volume 15, Issue 704
12 July 2023.

DOI: 10.1126/scitranslmed.abq3665

# Improved control of a prosthetic limb by surgically creating electro-neuromuscular constructs with implanted electrodes

Jan Zbinden[1,2], Paolo Sassu[1,3,4], Enzo Mastinu[1,2,5], Eric J. Earley[1,2], Maria Munoz-Novoa[1,6], Rickard Brånemark[7,8,9], Max Ortiz-Catalan[1,2,10*]

[1] Center for Bionics and Pain Research, Mölndal, Sweden.
[2] Department of Electrical Engineering, Chalmers University of Technology, Gothenburg, Sweden.
[3] Department of Hand Surgery, Sahlgrenska University Hospital, Mölndal, Sweden.
[4] Department of Orthoplastic, IRCCS Istituto Ortopedico Rizzoli, Bologna, Italy.
[5] The BioRobotics Institue, Scuola Superiore Sant'Anna, Pisa, Italy.
[6] Center for Advanced Reconstruction of Extremities, Sahlgrenska University Hospital, Mölndal, Sweden.
[7] Center for Extreme Bionics, Biomechatronics Group, MIT Media Lab, Massachusetts Institute of Technology, Cambridge, USA.
[8] Department of Orthopaedics, Gothenburg University, Gothenburg, Sweden.
[9] Integrum AB, Mölndal, Sweden
[10] Bionics Institute, Melbourne, Australia.

## One Sentence Summary

Surgically created electro-neuromuscular constructs allow for the intuitive control of all five fingers of a prosthetic hand after a transhumeral amputation.

## Abstract

Muscles remnant after amputation are the most common source of control signals for prosthetic hands. This is because myoelectric signals can be intuitively generated by the user at will. However, in higher amputation levels, such as transhumeral, not enough muscles are left to generate myoelectric signals to control the many lost joints, thus making intuitive control of

the prosthetic joints (*e.g.*, wrist and fingers) unattainable. Here, we show that severed nerves can be divided along their fascicles and redistributed to concurrently innervate different types of muscle targets, particularly native denervated muscles and non-vascularized free muscle grafts. We instrumented these neuromuscular constructs with implanted electrodes accessible via a permanent osseointegrated interface allowing for bidirectional communication with the prosthesis while also providing direct skeletal attachment. We found that the transferred nerves effectively innervated their new targets as proven by a gradual increase of myoelectric signal strength. This allowed for individual flexion and extension of all fingers of a prosthetic hand by a patient with a transhumeral amputation. Improved prosthetic function in tasks representative of daily life was also observed. This proof-of-concept indicates that the amount of motor neural commands can be considerably increased by creating electro-neuromuscular constructs using distributed nerve transfers to different types of muscle targets and implanted electrodes, and thus could enable the next generation of more highly integrated neuromusculoskeletal prostheses.

# Introduction

Upper limb amputation substantially changes the way in which one interacts with the environment, with the most proximal amputations suffering from the highest impairment as function decreases with every lost joint. Mechatronic joints can now be combined to replace limbs lost to amputations. However, commanding artificial joints in a similar manner to biological ones has remained challenging. Myoelectric signals extracted from residual muscles in the stump have been the preferred source of control in mechatronic prostheses (*a.k.a* myoelectric prostheses). The standard clinical solution is for prosthetic users to modulate the activity of an antagonistic pair of remanent muscles to drive the activation of a single degree of freedom (DoF) prosthetic joint. The problem is that there are not enough remanent muscles to drive several prosthetic joints in an intuitive manner. For example, the opening and closing of a prosthetic hand can be driven by the contraction of the biceps and triceps muscles in a transhumeral amputation, but no other muscles are left to control the prosthetic elbow, wrist, or individual fingers.

Surgically reconstructing the extremity can ameliorate the problem of insufficient control signals by creating new myoelectric sites . Nerve transfers to native but denervated muscles, also known as targeted muscle reinnervation (TMR) *(2)*, have gained popularity in the past decade. This procedure repurposes remnant muscles at the stump to amplify neural motor commands to the missing joints. This is achieved by denervating a muscle with dispensable biomechanical function, and then reinnervating it with a major nerve severed by the amputation (*i.e.*, a nerve transfer). Once the muscle has been reinnervated, electrodes on the surface of the skin can be used to record neural commands to the missing limb as the reinnervated muscles are large enough to electrically radiate transcutaneously. A downside of this approach is that all the motor information normally contained in the severed nerves is reduced to a single

myoelectric signal. Therefore, reconstruction with nerve transfer to native muscles has only allowed for up to six independent control signals *(3)*, which are enough to drive a mechatronic elbow, wrist, and end effector (each using a pair of signals/electrodes). However, dexterous manipulation of objects is out of reach with this approach as no additional information is left for individual finger control.

Recently, another surgical approach has been suggested in which rather than transferring the severed nerve to a native muscle, said nerve is longitudinally dissected into several fascicles and then each fascicle is wrapped with a free muscle graft. This strategy, also known as regenerative peripheral nerve interfaces (RPNIs) *(4, 5)*, aims at extracting more motor neural information at the cost of accessibility. Accessibility here is a problem because the free muscle grafts are too small to be recorded with surface electrodes, and thus the implementation of such an approach in prosthetic devices requires the use of implanted electrodes *(6)*. Implanted electrodes have shown to improve prosthetic control over their skin-surface non-invasive counterparts *(7–9)*, but bring an additional obstacle to clinical implementation, namely the need for a safe, reliable, and long-term stable transcutaneous interface between the implanted electrodes and the prosthesis *(10)*. The lack of such an interface has hindered the clinical adoption of implanted electrodes and the more refined surgical techniques for artificial limb replacement.

In this study, we present a novel combination of surgical reconstruction procedures combined with a long-term stable neuromusculoskeletal interface that allows for bidirectional communication between electro-neuromuscular constructs and the artificial limb (Figure 1). In a patient with a transhumeral amputation, we transected the neuromas of the three major nerves at the residual limb (median, ulnar, and radial), and then dissected each nerve longitudinally in two groups of fascicles. One group was transferred to reinnervate native muscles that we first denervated. Electrodes were then implanted in these (to be) reinnervated native muscles, as

well as in the other available unreconstructed muscles. The other group of fascicles was further dissected to expose individual fascicles that were then used to reinnervate free muscle grafts harvested from the lower limb. These grafts housed an intramuscular electrode each. These newly created electro-neuromuscular constructs were used to extract motor commands directed to the missing hand allowing for the intuitive flexion and extension control of all five fingers of a prosthetic hand in a patient with a transhumeral amputation (demonstration in Movie S1). In addition, improved prosthetic function while performing tasks normally found in daily life was also observed (demonstration in Movie S2).

# Results

## Surgical procedure and neuromusculoskeletal interface

A 51 years-old male who lost his left arm above the elbow due to a traumatic injury participated in this study. He was provided initially with a conventional myoelectric prosthesis using skin-surface electrodes but used it rarely due to discomfort related to the socket attachment. In addition, he was unsatisfied with the limited and unreliable myoelectric control provided by the surface electrodes. We addressed these problems with the combination of surgical reconstruction procedures together with an electromechanical interface for prosthesis attachment and bidirectional communication with implanted electrodes. This neuromusculoskeletal interface was implanted in three different stages. First, a titanium fixture was implanted intramedullary and left undisturbed to osseointegrate (Figure 1). Six months later, a percutaneous component (abutment, Figure 1) was coupled into the fixture allowing for the skeletal attachment of the prosthetic arm, thus addressing the patient's socket-related discomfort. The limited and unreliable prosthetic control was then addressed in a third surgery by reconstructing the neuromuscular structures within the residual limb and instrumenting them with implanted electrodes (Figure 1).

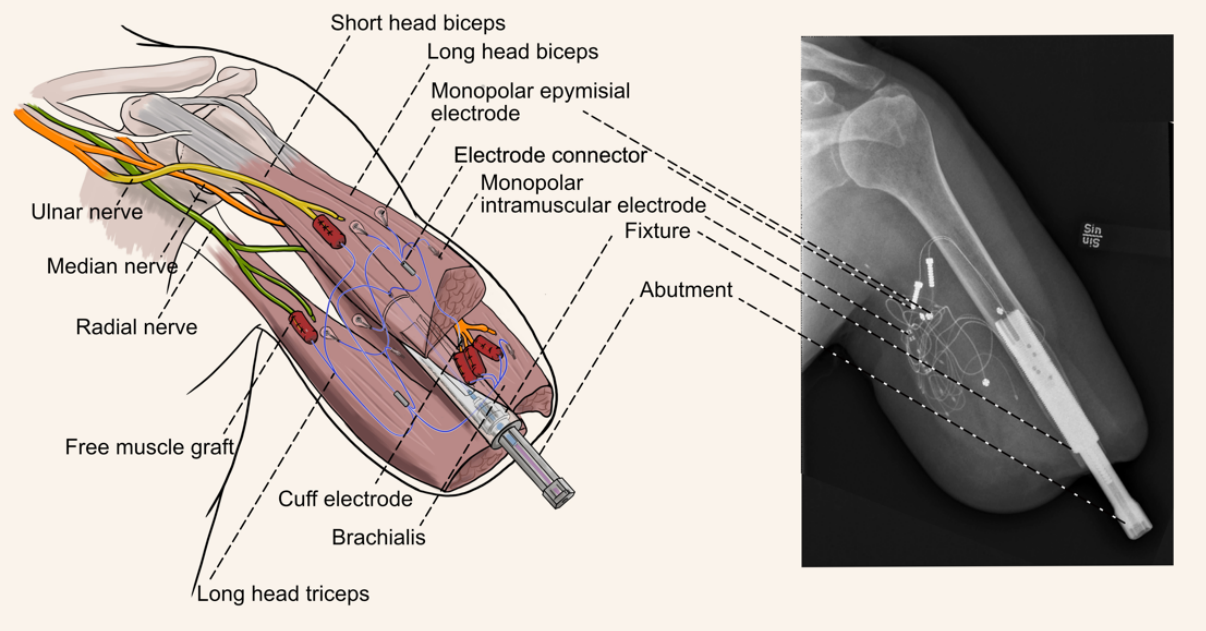


117

118 ***Figure 1 Schematic illustration and X-ray of a highly integrated human-machine interface.***

119

120 The median nerve was dissected longitudinally in four groups of fascicles to reinnervate the
121 brachialis muscle and three free muscle grafts (Figure 1). Similarly, the ulnar nerve was divided
122 into two parts to innervate the short head of the biceps muscle and one free muscle graft (Figure
123 1). The radial nerve was divided into two parts to then reinnervate the lateral head of the triceps
124 muscle and one free muscle graft (Figure 1). The neuromas located at the end of these nerves
125 were transected prior dissection and transfer. The non-vascularized muscle grafts were
126 obtained from the vastus lateralis muscle in the thigh.

127 Intramuscular electrodes were inserted in native muscles as well as in the free muscle grafts.
128 Epimysial electrodes were implanted on each head of the biceps muscle, and on the lateral and
129 long heads of the triceps muscle (Figure 1). A cuff electrode with a mixed-tripolar contact
130 configuration *(11)* was implanted around one of the fascicles of the median nerve (Figure 1).
131 Communication between the implanted electrodes and the outside of the body was achieved

through the osseointegrated implanted within which feedthrough mechanisms allowed for bidirectional signals transmission while sealing the interface *(9)*.

A revision surgery for the skin interface was performed to remove excess granulation tissue at week 65 post-implantation. The patient was treated with antibiotics after superficial skin infections at week 94, 135, and 171 post-implantation, and after a deep soft-tissue infection at week 116 post-implantation.

## Neuromusculoskeletal interface stability

The stability of the neuromusculoskeletal interface was examined by monitoring the electrical resistance of each implanted electrode over time. The resistance of the epimysial electrodes ranged between 1.3-1.9 kΩ at four-weeks post-implantation and stabilized at 1.4-1.6 kΩ (Figure 2a) two-years post-implantation. Similarly, the resistance of the intramuscular electrodes ranged between 250-1400 Ω at four-week and then 740-1300 Ω (Figure 2b) two-years after implantation. The cuff electrode has two types of contacts *(11)*: ring and discrete. The resistance of the ring contact was 1.5 kΩ at four-week and 1.5 kΩ two years post-implantation, and the resistance of the three discrete contacts ranged between 15-20 kΩ at four weeks and 5.1-14 kΩ after two years (Figure 2c). The resistance values for the intramuscular electrodes did not show a statistically significant change over time ($p = 0.41$). The resistance values of the epimysial and cuff electrodes decreased slightly during the second year ($p = 0.041$ and $p = 0.026$, respectively). One intramuscular electrode was considered an outlier and excluded from the aforementioned range and further analyses, since it increased from 1.3 kΩ to 141 kΩ between 40- and 127-weeks post-implantation. This abnormally large increment was most likely due to damage to the external connector pin. For an overview of all resistance values see Tables S1.

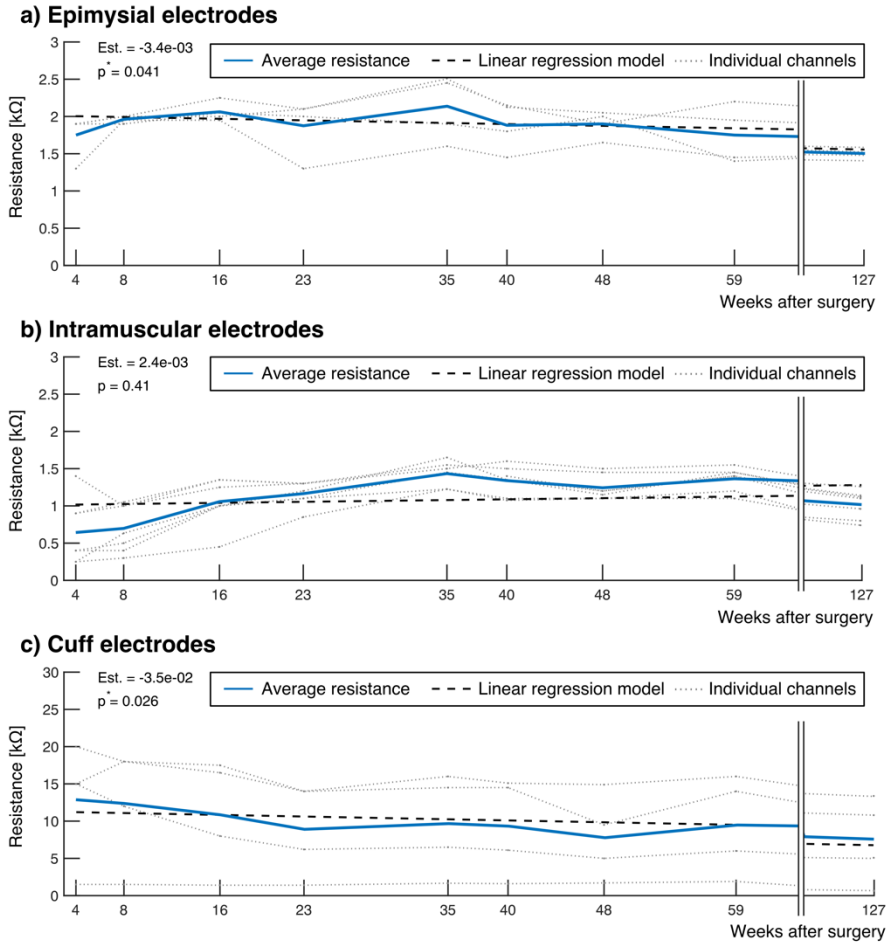


***Figure 2 Electrical resistance of epimysial, intramuscular, and cuff electrodes over time.*** *(a) Resistance of the epimysial electrodes on unreconstructed and reinnervated native muscles (n=4). (b) Resistance of the intramuscular electrodes in unreconstructed muscles, reinnervated native muscles, and reinnervated free muscle grafts (n=8). (c) Resistance of the ring and three discrete contacts the cuff electrode around a fascicle of the median nerve (n=4). The parameter Est. denotes the slope of the linear regression.*

## Reinnervation development and myoelectric signals quality

The development of the signal quality of the different implanted electrodes was quantified by calculating the signal-to-noise ratio (SNR). As expected, weeks were required for the functional reinnervation of all muscular constructs, as opposed to the unreconstructed muscles from which electromyographic (EMG) activity was readily available directly after implantation. Relevant signs of reinnervation were observed 23 weeks post-implantation

(examples in Figure 3). Exceptions were the muscles reinnervated by the radial and median nerves, which began to display information about single finger actuation at around 40 weeks post-implantation.

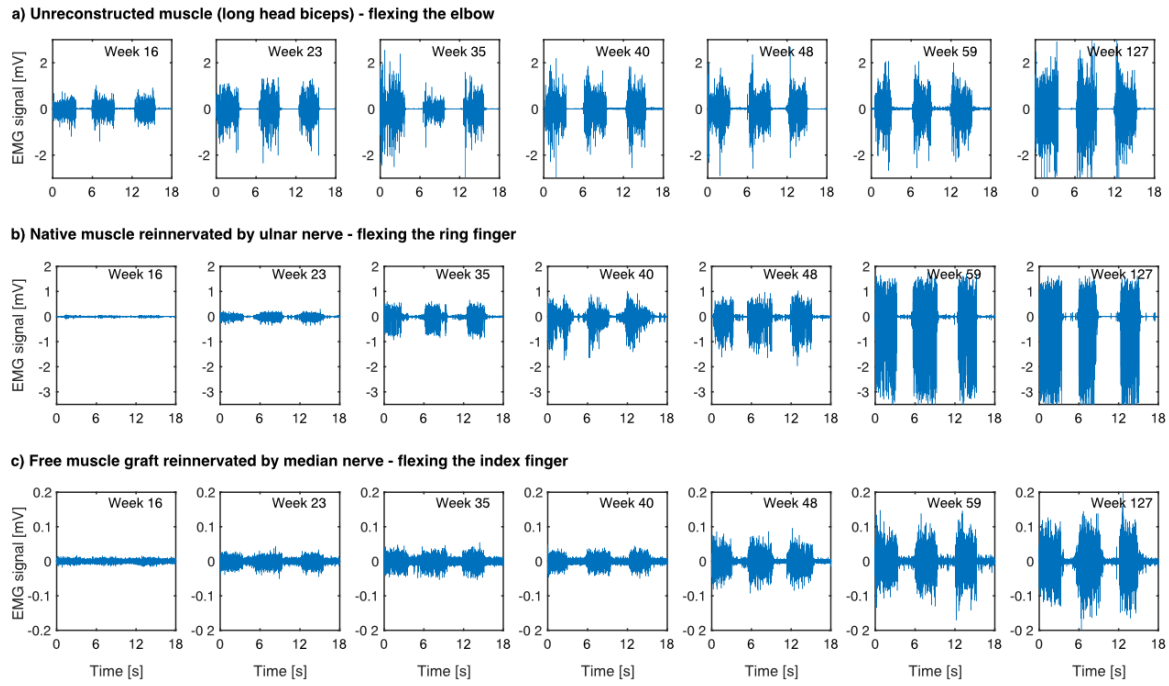


***Figure 3 Representative examples of the raw EMG signals over time.*** *(a) Raw EMG signals for electrodes in an unreconstructed muscle, (b) a reinnervated native muscles, and (c) a free muscle graft. Each EMG recording consists of three seconds sequences of three active movement and rest periods.*

Soon after the surgery, the four electrodes placed in unreconstructed muscles displayed an average SNR of 23.3± 6.1dB (Figure 4a) and remained nearly constant over time with an average SNR of 24.1± 5.4dB at the end of the experiment period. The average SNR of the three electrodes in the reinnervated native muscles started at 1.6±5.4 dB and increased to 19.4±6.4 dB (Figure 4b). All three electrodes in reinnervated muscles showed a significant increase in SNR over the 127 weeks of experimental period ($p$ = 5.8e-9, $p$ = 3.8e-6, and $p$ = 1.3e-4 for the radial, ulnar, and median electrodes, respectively). The electrodes in the five free muscle grafts started with an average SNR of 1±0.8 dB and developed up to an average SNR

of 17.8±2.4 dB (see Figure 4c). A significant SNR increase was observed over the two-year period since electrode implantation for the radial ($p$ = 2.7e-11), ulnar ($p$ = 8.4e-10), and the three median electrodes ($p$ = 2.4e-14, $p$ = 9.3e-5, $p$ = 1.5e-7, respectively). For an overview of all SNR values see Tables S2.

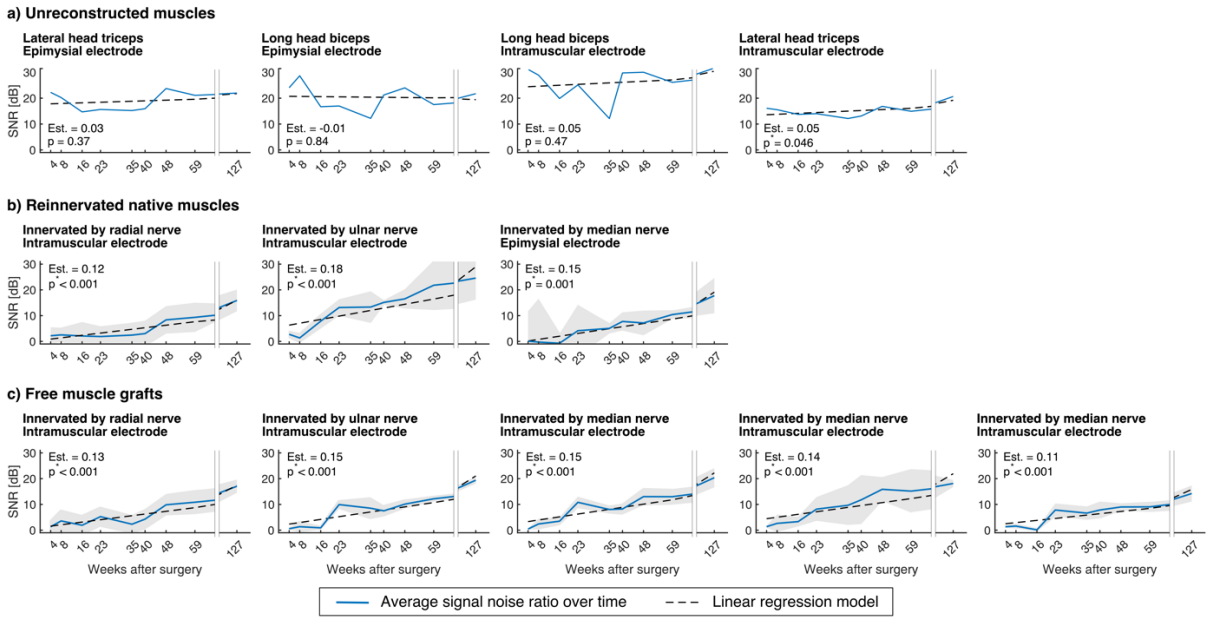


***Figure 4 Signal to noise ratio development over time.*** *Change of signal to noise ratio of (a) four electrodes in unreconstructed muscles (n=1 movement), (b) three electrodes on/in reinnervated native muscles (n=6, n=3, and n=4 movements from left to right, respectively), and (c) five electrodes within reinnervated free muscle grafts (n=6, n=3, n=5, n=3, and n=3 movements, from left to right, respectively). The grey areas depict the standard deviation around the average values over the number of movements. For all signal to noise ratio calculations, only data of the main movements that anatomically corresponded to the electrode placement/innervation site were considered (see Methods for more details). The parameter Est. denotes the slope of the linear regression,*

## Decoding of motor volition

We decoded the intended movements of the missing arm and hand in two groups: nine gross movements and eleven finger movements. Gross movements consisted of hand open/close, wrist pro/supination, wrist flexion/extension, elbow flexion/extension, and no movement (rest). Finger movements consisted of all five fingers flexion/extension and no movement. We used information from all electrodes to compute offline and real-time classification performance by

Linear Discriminant Analysis. The *Motion Test (2)* as implemented in the open source platform BioPatRec *(12)* was used to evaluate offline and real-time decoding.

## Gross movements

The offline accuracy steadily increased within the first 23 weeks after implantation and remained between 95.8% and 99.3% (see Figure 5a). The patient successfully completed the *Motion Test* with gross movements for the first time 16 weeks post-implantation (see Figure 5b). Over the duration of the experiment, the completion time for a single gross movement decreased from 4.0±0.1 s to 1.8±0.7 s with a minimum of 1.2±0.2 s (see Figure 5c). Correspondingly, the online accuracy of classifying all eight gross movements increased significantly from 36±4% to 66±16% ($p$ = 0.005), with a maximum of 75% 48 weeks after implantation (See Figure 5d). For an overview of the Motion Test metrics for gross movements see Tables S3.

## Single finger movements

The offline accuracy increased within the first 16 weeks and then remained between 86.7-96.8% over the next two years (see Figure 5e). The average completion rate of the *Motion Test* for single finger decoding increased from 13±35% to 100% between the first and the last training session (see Figure 5f). The average time for completion significantly decreased ($p$ = 0.05) from 7.0±0.6 s down to 1.6±0.6 s (see Figure 5g). The average online classification accuracy increased significantly ($p$ = 1.9e-5) from 6±3% to 69±6% (see Figure 5h). For an overview of the Motion Test metrics for finger movements see Tables S4.

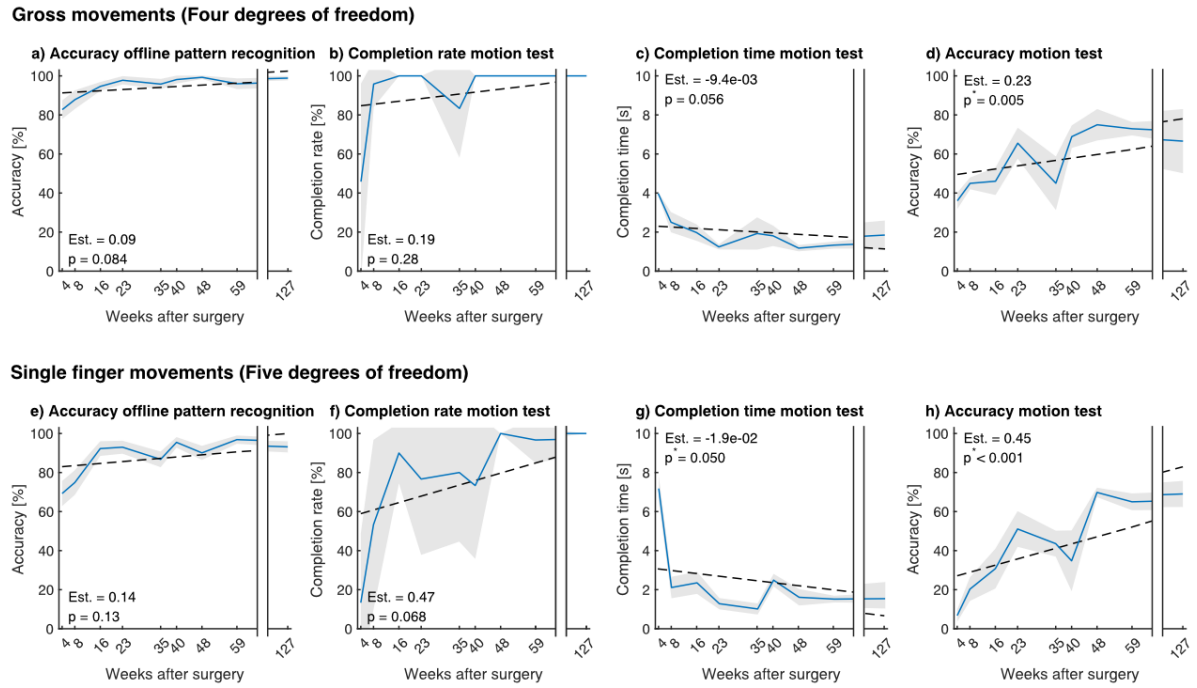


***Figure 5 Offline and online decoding performance.*** *Decoding performance using gross (hand open/close, supination/pronation, wrist flexion/extension, and elbow flexion/extension) and single finger movements over a two-year period. (a) Offline accuracy of nine gross movements (n = 9 movements, 100 repetitions). (b) Motion test completion rate for gross movements (n = 9 movements, 3 trials), where 100% indicates that all required movements were performed. (c) Completion time (time between the first decoded movement and twenty correct predictions of the promoted movement) and (d) accuracy (percentage of correct predictions) for the four degrees of freedom during the motion test. (e) Offline accuracy of individual fingers (n = 11 movements, 100 repetitions). (f) Completion rate, (g) completion time, and (h) accuracy for the motion test for individual finger decoding (n = 11 movements, 3 trials each). The parameter Est. denotes the slope of the linear regression.*

## Functional outcomes

We measured prosthetic function using the Assessment of Capacity for Myoelectric Control (ACMC) *(13)* and found it to improve by 16.7% at 59 weeks after the intervention (32.2 to 37.6, see Figure 6a) using intuitive control with signals from the newly created myoelectric sites. Worthy of notice is that no improvement was observed earlier at 8 weeks after the intervention (32.2 to 30.3, see Figure 6a) using nonintuitive control with signals from

unreconstructed native muscles. The ACMC was performed using a conventional prosthesis with socket attachment and surface electrodes before the intervention, and skeletal attachment and implanted electrodes after the intervention. The prosthesis consisted of a single degree-of-freedom (DoF) myoelectric hand (MyoHand VariPlus Speed, Ottobock) and an elbow (ErgoArm, Ottobock) with a myoelectric locking system (1.5 DoF combined). When taking advantage of all the myoelectric sites by using a 4.5 DoF control scheme (allowing for simultaneous and proportional control of the thumb, index finger, middle/ring/little fingers, wrist rotation, and elbow lock/unlock), the patient achieved the highest improvement at 39.8% (45.0 ACMC score, Figure 6b). This was despite using such a system for the first time (untrained). The 4.5 DoF prosthesis consisted of a multi articulated myoelectric hand (BeBionic, Ottobock), a wrist rotator (Ottobock), and an elbow (ErgoArm, Ottobock) with a myoelectric locking system. Conversely, the Southampton Hand Assessment Procedure (SHAP) score improved both at 8 and 59 weeks after intervention by 42.6% and 82.7%, respectively (24.9 to 35.5 and 45.8, Figure 6c). Using the 4.5 DoF control scheme with the electro-neuromuscular constructs, the SHAP scored doubled to 50.1 (101.2%) compared to conventional surface electrodes (see Figure 6d). For an overview of the functional outcome values see Tables S5.

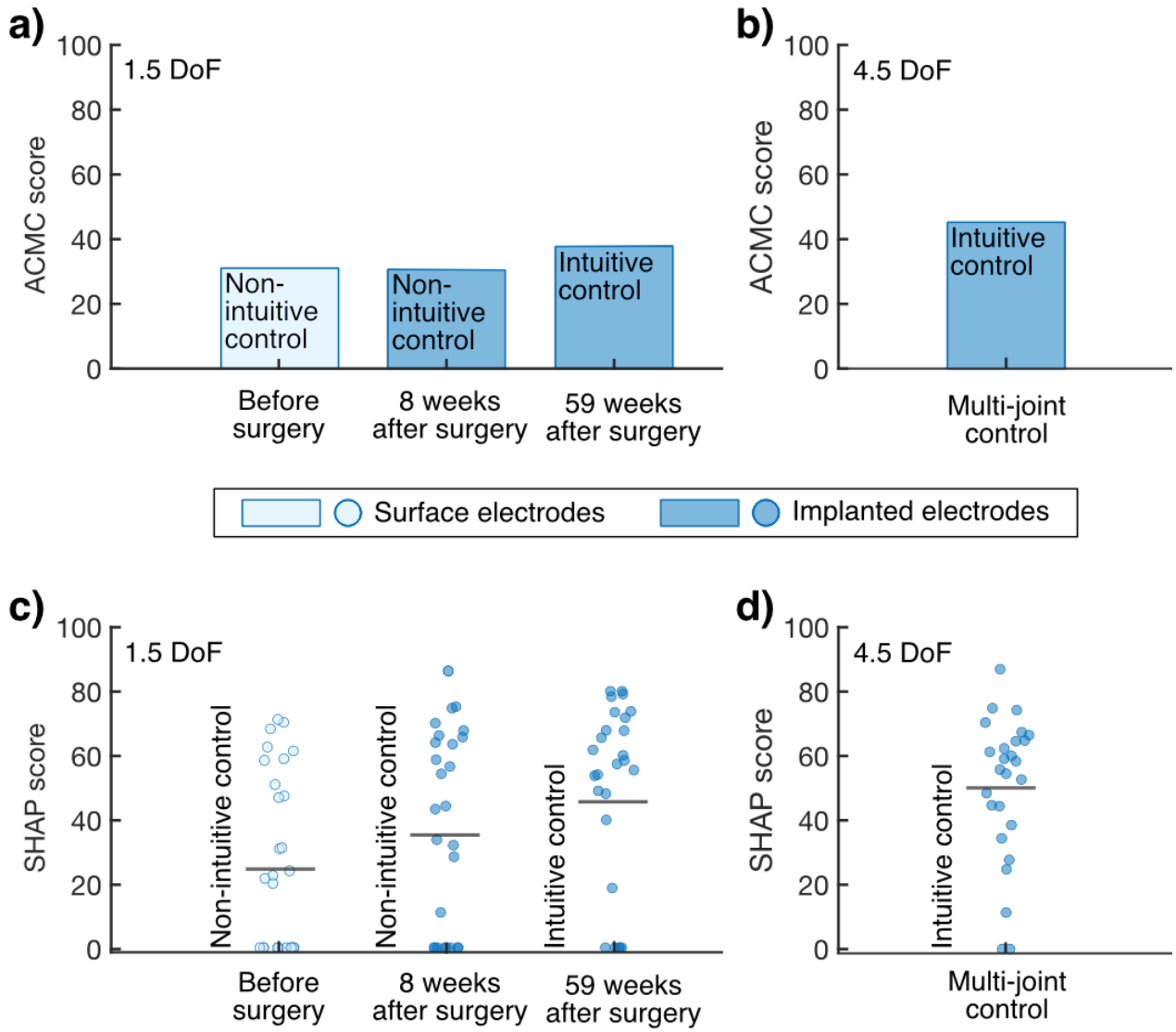


***Figure 6 Results of functional tests.*** *(a) ACMC outcome, scored between 0 and 100, for a 1.5 DoF control scheme using surface electrodes before surgery and implanted electrodes at week 8 and 59 after surgery. A higher score indicates a higher capacity for myoelectric control. (b) ACMC outcome when using a 4.5 DoF simultaneous and proportional control scheme with the electro-neuromuscular constructs and without prior training. (c) Outcome of SHAP for surface electrodes before surgery and implanted electrodes at week 8 and 59 after surgery. The circles indicate the linear Index of Function, scored between 0 and 100, for each task of the SHAP (n = 26 tasks). The horizontal black line shows the weighted linear Index of Function (W-LIOF), where a higher score represents greater prosthetic functionality during activities of daily living. (d) Outcome of SHAP (n = 26 tasks) when using a 4.5 DoF simultaneous and proportional control scheme with the electro-neuromuscular constructs and without prior training.*

# Discussion

In this study, we present a novel combination of surgical reconstruction procedures together with a long-term stable neuromusculoskeletal interface. Thanks to the wired access to the implanted electrodes provided by the neuromusculoskeletal interface, it was possible to track the signals development over a period of two years. The signals development was analyzed in terms of stability (*i.e.*, electrical resistance), quality (*i.e.*, signal-to-noise ratio), and feasibility for advanced prosthetic control based on myoelectric pattern recognition (offline and in real-time decoding). Aside from confirming the long-term stability of the interface and remarkable strengthening of the myoelectric signals over time, we have shown that nerve transfer to denervated native muscles, and non-vascularized free grafted muscles, increased the number of myoelectric sources for prosthetic control to ultimately allow for independent control of all five fingers (demonstration in S1 Movie).

The main limitation of our study is that only one patient was treated with this new surgical approach. Here, we did not aim at comparing the surgical nerve transfer to native muscles versus free muscle grafts, but rather to evaluate the feasibility of doing this concurrently. Worthy of notice is that even if the nerve transfers would have not been successful, the patient would have still enjoyed improved prosthetic control and sensory feedback using unreconstructed sites *(7, 14)*, which was an important ethical aspect to be considered in this investigation.

The final number of reinnervation sites depended on the number of fascicles that can be dissected without compromising naturally occurring fascicle crossings within the nerve trunk. Larger diameter nerves, such as the median nerve, allow for more dissectible fascicles (four in our study) than smaller ones, such as the radial nerve (two fascicles in our study). The number of dissectible fascicles can vary from person to person and the level of amputation. Electrode

selection, on the other hand, depends on the type of muscular target. The free muscle grafts are non-vascularized and are therefore dependent on blood diffusion from surrounding tissue for survival, albeit vessels within the innervating fascicle can also contribute. Placing an epimysial electrode would compromise blood diffusion in a relatively large surface area, and therefore intramuscular electrodes are preferred for this muscular target. Native muscles are vascularized and both epimysial and intramuscular electrodes have been employed successfully in this case.

We use the electric resistance to each electrode as a metric of long-term stability of the interface as extreme high or low values would indicate an interruption of continuity (open circuit) or a loss of independent connection (short circuit), respectively. Both scenarios would compromise the use of the implanted electrodes and interface for prosthetic control. We found that the electrical resistance of the implanted electrodes (including leads and feedthrough connectors) remained stable within functional bounds. These results are in accordance with the long-term electrical stability of previously-reported subjects that received neuromusculoskeletal interfaces *(7, 9)*.

We found that the transected nerves effectively innervated the native muscles and free muscle grafts at about 5 months (ulnar and median nerves) and 11 months (radial nerve) post-surgery. The innervation process led to distinct myoelectric signals appearing on the different electrodes and a notable increase in SNR. As expected, the epimysial electrodes placed on unreconstructed native muscles, not having to reinnervate, featured myoelectric signal activity soon after the surgery and exhibited a stable and slightly increasing SNR over the whole 127 weeks.

In a previous study with two patients with transhumeral amputation *(15)*, we tracked the reinnervation of the radial and ulnar nerves into denervated native muscles reaching an average

317 SNR of 20 dB and 26 dB, respectively. Here, we report an average of 19.4 dB for similarly
318 reinnervated native muscles, despite using monopolar as opposed to bipolar electrodes as in
319 our previous study. When restricted on the number of possible electrode contacts in an implant
320 system, using monopolar electrodes allows for instrumenting more targets with the downside
321 of reducing SNR as compared with a bipolar configuration. Our results indicate that this is an
322 acceptable tradeoff when considering that more information can be obtained by adopting a
323 monopolar strategy.

324 In a study by Vu *et al. (6)*, seven patients with upper limb amputation underwent RPNI surgery
325 for the treatment of neuroma pain. Three of their patients were implanted with intramuscular
326 electrodes with percutaneous leads one to three years after surgery. They reported an average
327 SNR of 4.2 dB with fine wire electrodes, 68.9 dB (after a three-year reinnervation period), and
328 21.0 dB (after a one-year reinnervation period) with intramuscular bipolar electrodes. These
329 SNR values are comparable with our findings for similarly reinnervated free muscle grafts at
330 two-years after surgery despite using monopolar electrodes (max. 21.7 dB, average 17.8 dB),
331 and therefore expecting lower SNR values compared to a bipolar configuration.

332 The two patients with intramuscular electrodes in native and reconstructed muscles in Vu *et*
333 *al.*'s study were able to control some finger movements (thumb, ring finger, and small finger
334 flexion, thumb opposition, and concurrent ab- and ad-duction of all fingers) albeit limited to
335 four movements at the time *(6)*. These patients had transradial amputations and therefore some
336 of the native muscles responsible for finger control were available, as opposed to a
337 transhumeral amputation where all muscles related to finger control are lost. For a person with
338 a transhumeral amputation that underwent TMR, Osborn *et al. (16)* demonstrated in a video
339 recording the real-time individual flexion of up to three fingers at the time, with combined
340 extension, effectively decoding four movements. In comparison to these studies, we believe
341 that the considerable increase in prosthetic control reported here (independent flexion and

extension of all five fingers) was made possible by combining different surgical techniques and thereby creating notably more sources for myoelectric control.

Over the duration of our investigation, the patient's ability to differentiate hand movements improved steadily. Our patient successfully completed *Motion Tests* with gross movements (4-DoF) already 16 weeks post-implantation, with faster completion times and increasing accuracy over time. Concurrently with the innervation of the radial nerve, the subject completed the *Motion Test* with single finger movement (5-DoF) at 48 weeks post-implantation. Similar completion times and accuracies were achieved in both sets of movements (gross and single fingers).

Kuiken *et al*. performed TMR surgery on five subjects (three with shoulder disarticulation and two with transhumeral amputation) and investigated real-time decoding of ten elbow, wrist, and hand movements using surface electrodes *(2)*. They reported an average offline classification accuracy of 95 % and *Motion Test* completion rates of 86.9 % and 96.3 % with completion times of 1.54 s and 1.29 s, for four hand movements and for six elbow and wrist movements, respectively. Another study by Cipriani *et al.* also demonstrated the feasibility of real-time finger control *(17)*, albeit in transradial amputees as opposed to transhumeral. They reported the decoding of seven movements, four of which were flexing individual fingers, with an average *Motion Test* completion rate of 79±16 %. In comparison with these studies, we assume that our patient was able to achieve higher completion rates (100%) owing to the combination of surgical reconstruction and permanently implanted electrodes.

Reliability in daily use has been reported as the main factor for prosthesis acceptance *(18)*. And at a first glance, our reported *Motion Test* accuracy (69-75%) might suggest low reliability, despite being higher than previously reported to yield acceptable controllability *(19)*. It is worth noticing that decoding accuracy is not synonymous with controllability. Spurious

misclassifications are common in decoders but do not translate necessarily to noticeable errors during prosthetic control as classification output is continuously overwritten and low-pass filtered by the motors in the prosthesis. For the *Motion Test* experiment, the patient was asked to perform pre-selected movements intuitively during the recording session, without prior training of the movements. Exploring the signal space together with the patient to find and train more distinguishable, yet still intuitive, signal patterns for the different movements would likely lead to an improvement in decoding consistency.

The pre-defined movements for the *Motion Test* experiment were selected to showcase the potential of the surgical reconstruction approach. To increase reliability during home-use, a subset of all the movements can be chosen instead. For example, only actuating the thumb and index finger individually and actuating the middle, ring, and little finger as one movement decreases the complexity of control drastically while still offering considerable functional improvements.

A sequential decoding scheme, meaning that only one movement is output at the time, limits functionality during home-use. Simultaneous control would increase the functional benefits during home use, especially for finger movements (closing individual fingers sequentially to perform a grasp would be slow, unintuitive, and frustrating). Adding proportionality could further contribute to reliability and intuitiveness.

Based on the above-described considerations, we used a 4.5 DoF (thumb, index finger, middle/ring/little fingers, wrist rotation, and elbow lock/unlock) simultaneous and proportional control scheme to evaluate the functional benefits of a higher DoF controller made possible by the additional myoelectric sources created by the surgical reconstruction. The use of the neuromusculoskeletal prosthesis resulted in an increase of 12.8 points (however, the minimum detectable change is 14.5 points *(20)*) from 32.2 to 45.0 during the ACMC, and a doubling of

390 the SHAP score from 24.9 to 50.1 compared to the standard two-site surface EMG electrode
391 prosthesis used prior to the surgical intervention. Even when using the same control scheme
392 (1.5 DoF direct control), the intuitive control and the added reliability from having the
393 electrodes implanted led to an increase in prosthetic functionality (ACMC score increased from
394 32.2 to 37.6 and the SHAP score increase from 24.9 to 45.8) compared to the two-site surface
395 electrode prosthesis used before the intervention. These results indicate that electro-
396 neuromuscular constructs using implanted electrodes can lead to greater capacity for
397 myoelectric control and thereby functionality for everyday tasks (demonstration in S2 Movie).

398 The improvements in functionality were achieved despite the patient only having used such a
399 prosthesis for a couple of hours. We therefore assume that the intuitive control granted by the
400 newly created myoelectric sources greatly facilitated learning a more complex control scheme.
401 Given the improvement in functionality we observed when the patient used the 1.5 DoF
402 prosthesis over an extended time at home, we foresee that prolonged use of the 4.5 DoF
403 prosthesis could lead to further functional improvements to facilitate activities of the daily life.

404 Due to constraints on the patient's availability, we performed only one set of functional tests
405 during each follow-up. Therefore, a limitation of our study is that we did not disentangle the
406 separate contributions to improvement of 1) electrode type (surface vs implanted); 2)
407 intuitiveness of control (native residual muscles vs surgically reconstructed myoelectric sites);
408 and 3) potential learning effects *(21)*. The SHAP but not the ACMC scores showed
409 improvement early post-intervention when the control scheme was non-intuitive, and both
410 scores showed improvement later at week 59, when the control was intuitive using the new
411 surgically reconstructed myoelectric sites and the patient was more experienced. Further
412 systematic work is needed to disentangle the contribution of each variable.

We observed undesired crosstalk between myoelectric sites that can be attributed to several causes, such as the placement of the electrodes; the location of the electro-neuromuscular constructs; the use of monopolar electrodes; and the nature of the neuromuscular constructs themselves as they often share neural information related to the same movements. Greater attention to the placement of electrodes and neuromuscular constructs can reduce signals crosstalk, but not entirely. Intraoperative identification of nerve fascicles during reconstruction remains challenging but achieving such a deed would considerably improve the creation of optimal neuromuscular control sources. On the engineering side, recent advances in source separation algorithms have shown to be a promising approach for decoding movement intent, offering insights into the discharge patterns of motor neurons *(22, 23)*. Indeed, it has been shown that neural and myoelectric information can be combined to achieve more independent control of different prosthetic joints *(24, 25)*.

In this proof-of-concept study, we have demonstrated the feasibility of transferring severed nerves to native muscles and free muscles grafts, resulting in long-term stable electro-neuromuscular constructs using implanted electrodes that can be safely and reliably accessed using a neuromusculoskeletal interface. Safety and reliability are prerequisites for the clinical implementation of new prosthetic technologies. By merging surgical and engineering technologies, our approach allows for a more comfortable use of the prosthesis *(26)*, for a more functional load transfer between the prosthesis and the skeleton *(27, 28)*, for a more reliable and precise control of the prosthesis *(8, 9)*, and opens possibilities for a more advanced and dexterous control of a prosthetic hand supported by tactile sensory feedback *(9, 29)*. This research contributes to the wider clinical application of osseointegration and advanced surgical reconstructions to improve artificial limb replacement.

# Materials and Methods

## Study design

This single-person case study investigated if creating electro-neuromuscular constructs using distributed nerve transfers to different types of muscle targets instrumented with implanted electrodes can increase the number of myoelectric sources for prosthetic control. The main pre-specified study objective was to assess if additional myoelectric sources could be created by transferring nerves to native and free grafted muscles and be used to decode motor volition (as measured by the Motion Test). The secondary pre-specified objective was to assess the innervation and development of the different surgical constructs over time (measured by the signal to noise ratio (SNR) over time). In addition, we evaluated prosthetic function during tasks representative of daily life (measured by the ACMC and SHAP).

One patient with a transhumeral amputation due to a traumatic injury (July 2015) participated in this study. The first surgical stage, implanting the titanium fixture, was performed in September 2017. The percutaneous component of the implant system was coupled into the fixture in February 2018. And the third surgical stage (the basis for the presented study), reconstructing the neuromuscular structures within the stump and instrumenting them with electrodes, was performed in December 2018.

The study was designed to collect data over a period of one year at eight periodic follow-ups (7.8±2.9 weeks between lab visits) and at a follow-up two years (127 weeks) after reconstruction and electrode implantation. Functional outcome data was collected before surgery and at 8 and 59 weeks after the surgery. An additional round of functional tests with a multi-DoF prosthesis was conducted 215 weeks after surgery as requested during the peer-review process of this article.

During the time of this two-year study, the patient first used a prosthesis allowing for 1.5 DoF (hand open/close and elbow lock/unlock) for daily home-use. At week 65, the patient was fitted with an additional DoF (pronation/supination) *(21)*. 181 weeks after the surgery, the patient was also provided with an active elbow, allowing him to control a total of 3 DoF for daily home-use. In all cases, a direct control approach was used, allowing for simultaneous and proportional control of the individual DoF.

The study protocols were carried out in accordance with the declaration of Helsinki. The signed informed consent was obtained before conducting the experiments. The study was approved by the Regional Ethical Review Board in Gothenburg (Dnr. 18-T125).

## Surgical reconstruction and implantation

The radial nerve was exposed through a curvilinear incision proximally in the arm at its exit from the triangular interval. Branches to the lateral, long, and medial heads of the triceps were identified with the help of a nerve stimulator and isolated. The motor branch to the lateral head of the triceps was left intact, whereas the main branch to the long head was severed 5 mm before its entrance into the muscle and marked for later neurotization.

The main trunk of the radial nerve was then followed distalward and its stump retracted proximally. Once the large end neuroma was excised, the healthy-looking fascicles were split longitudinally into two halves. One half was anastomosed to the motor branch supplying the long head of the triceps. The other half lay in the center of a non-vascularized muscle graft which was folded around the nerve following the principle of an RPNI *(4, 5)*.

An anterior curvilinear incision in the arm gave access to the two major nerves, median and ulnar, as well as the musculocutaneous nerve that was identified in the groove between the long

and short heads of the biceps muscle. The long head maintained its original innervation whereas the motor branch of the short head was severed 5 mm before its entrance into the muscle. The distal stump of the ulnar nerve was identified, retracted proximally, and its neuroma excised. Similarly, to the radial nerve, the ulnar nerve was split longitudinally into two halves: one was sutured to the motor branch of the short head of the biceps, and the remaining half was placed in a non-vascularized muscle graft.

The distal stump of the median nerve was identified and retracted proximally, and the large neuroma stump was excised. The nerve was divided longitudinally into four groups of fascicles: one was reserved for sensory feedback and wrapped with an extraneural electrode; the remaining three were utilized to reinnervate non-vascularized muscle grafts. All the free muscle grafts were harvested from the vastus lateralis muscle in the homolateral thigh and had a standard dimension of 5X3X1.5 cm.

### Neuromusculoskeletal interface stability

The stability of the neuromusculoskeletal interface was examined over time by monitoring the electrical resistance of each implanted electrode. The resistance was computed by applying Ohm's Law to the voltage caused by a single current-controlled electrical pulse with known parameters (100 or 200 μA current amplitude and 100μs pulse width). The voltage was measured via an oscilloscope and an isolated differential probe.

### Myoelectric signals acquisition

During each follow-up, two EMG recording sessions were performed from all implanted muscular electrodes. The recording sessions were performed using BioPatRec *(12)*, an open-source platform for research on myoelectric pattern recognition, and the Artificial Limb Controller, an embedded system for controlling prosthetic devices *(30)*. EMG monopolar data

505 was sampled at 500 Hz with 16-bit resolution and online high-pass and notch filtered at 20 Hz
506 and 50 Hz, respectively.

507 For each recording session, the subject was asked to comfortably sit in front of a computer and
508 follow on-screen instructions to perform a pre-selected set of movements. This study focused
509 on two different sets of movements, defined as "gross" and "single finger" movements. The
510 gross movements set included open and close hand, supination and pronation, flex and extend
511 wrist, and flex and extend elbow. The single finger movements set included flexion and
512 extension of all digits, *i.e.*, thumb, index, middle, ring and pinky fingers. For every set, each
513 movement was repeated three times, alternating 3s of muscular effort and 3s of resting time.
514 The subject was asked to perform each movement at approximately 70% of maximum
515 voluntary contraction.

516

517 ## Myoelectric signals quality

518 The development of the signal quality of the different implanted electrodes was quantified by
519 calculating the signal-to-noise ratio (SNR). For each recorded channel, the recording session
520 was divided into segments containing the voluntary contraction information of each movement,
521 and segments containing the resting state signal. Solely the steady-state of the EMG signal was
522 considered, thus the SNR was calculated on the middle 70% samples of each segment (see
523 Mastinu *et al.* for a similar approach *(15)*). Furthermore, only the movement data that
524 anatomically corresponded to the electrode placement was considered to calculate the SNR of
525 each of the individual electrodes. For calculating the SNR of the two electrodes on/in the
526 unreconstructed lateral head triceps only the recorded elbow extension movement, and for the
527 two electrodes on/in the unreconstructed long head biceps, only the recorded elbow flexion
528 movement were used. For the electrodes placed on/in sites innervated by fascicles of the radial

nerve, recordings of pronation, extend elbow and extension of all fingers were used if activation was present. Hand, ring finger and pinky flexion movements were used to calculate the signal to noise ratio values of the electrodes on/in sites innervated by fascicles of the ulnar nerve. For the electrodes in sites innervated by fascicles of the median nerve, supination, hand flexion as well as thumb, index finger, and middle finger flexion were considered if activation was present. Finally, the root-mean-square values were calculated and then the SNR was obtained according to the formula *(1)*:

$$SNR_{dB} = 10 * \log_{10} \frac{EMG^2_{RMS,Movement(s)}}{EMG^2_{RMS,Rest}} \quad (1)$$

We considered native muscles and free muscle grafts to be effectively innervated at a sustained SNR of four and higher.

## Myoelectric pattern recognition

### Offline pattern recognition accuracy

The EMG data from the recording sessions was segmented into overlapping time windows of 200 ms (50 ms time increment). The Hudgins' set of features *(31)* (mean absolute value, zero crossing, waveform length, and slope changes) was extracted from each time segment. The obtained features were randomly divided into training, validation, and test sets with a ratio of 40%, 20%, and 40%, respectively. Then, these sets were fed to a Linear Discriminant Analysis (LDA) classifier for supervised training. Finally, the training was repeated 100 times and the resulting averages, for both sets of movements, were reported.

## Real-time pattern recognition accuracy

The real-time classification accuracy was assessed via the *Motion Test* introduced by Kuiken *et al. (2)* as implemented in BioPatRec *(12)*. In this test, the subject was asked to perform movements randomly prompted on a screen. For every requested movement, 20 non-contiguous classifications had to be correct within 10 seconds to deem the particular movement completed. From this, several metrics were calculated:

- Completion Rate as the percentage of completed motions,
- Completion Time as the time between the first correct prediction and the completion of the motion
- Real-time accuracy as the percentage of correct predictions over the total number of predictions during the completion time.

The Motion Test was repeated three times for each set of movements, gross and single finger movements. The average results and standard deviation over the three trials are reported.

## Functional outcomes

Prosthetic functionality was evaluated before and after the surgical intervention using the Assessment of Capacity for Myoelectric Control (ACMC)*(13)* and the Southampton Hand Assessment Procedure (SHAP)*(32)*. The ACMC measures a person's ability to perform daily tasks, scoring 22 aspects of prosthetic use on a 4-point rating scale with a maximum of 66 points per task. A normed composite score between 0-100 can be obtained from the raw score via Rasch analysis, where a composite score above 57.2 is classified as "extremely capable". The SHAP consists of two parts: the first part involves 12 tasks where the subject grasps and relocates abstract-shaped objects and the second part involves 14 tasks of activities of daily living (ADLs), such as turning a door handle, unbuttoning a shirt, and opening a jar. The

execution times of all 26 tasks are used to calculate the weighted linear Index of Function (W-LIF), a normed score where a score of 100 indicates normal hand function *(33)*.

The patient's habitual two-site surface EMG electrode prosthesis (one electrode pair placed on the bicep and triceps, respectively) with a direct control scheme was used for the pre-operative tests, while the neuromusculoskeletal interface was used for post-operative tests.

A 1.5 DoF direct control scheme based on electrodes in the native biceps and triceps (i.e., non-intuitive control) was used to control the prosthesis for the tests at 8 weeks after surgery. And at 59 weeks after surgery, a 1.5 DoF direct control scheme based on signals from the surgically created myoelectric sites was used to allow for intuitive opening (mapped to the signal from a free muscle graft reinnervated by median nerve) and closing (mapped to the signal from a native muscle reinnervated by ulnar nerve) of the prosthetic hand and lock/unlocking of the elbow (mapped to the signal from the native biceps). In both cases, the patient used the same control during daily life prior to the tests.

To demonstrate the functional benefits of the higher DoF controllers, the patient also performed the tests using a 4.5 DoF simultaneous and proportional controller. The 4.5 DoF controller allowed individual control of the thumb, index finger, middle/ring/little fingers, wrist rotation, and elbow lock/unlock. For example, simultaneous activation of the thumb and index allowed the patient to pinch, and simultaneous movement of all fingers allowed for hand opening and closing. The control scheme was comprised of a multi-layer feed forward neural network capable of multi-label classification *(19)* and a post-hoc proportionality algorithm taking the predicted class and the current mean absolute value into account. Prosthetic function with the 4.5 DoF controller was tested without prior training.

### Statistical analysis

To evaluate the development of the electrode impedance, the signals quality, and the offline and real-time pattern recognition accuracies over time, we performed a linear regression analysis as implemented in the "*fitlm*" function of MATLAB's Statistics toolbox (Mathworks, USA). For each linear regression analysis, we report the estimate (the slope of the linear regression) and the *p*-value (outcome of the *t*-statistic with the hypothesis test that the estimate is different to zero).

## List of Supplementary Materials

Table S1. Overview of electrical resistance of epimysial, intramuscular, and cuff electrodes over time

Table S2. Overview signal to noise ratio development over time

Table S3. Overview of offline and online decoding performance of gross movements

Table S4. Overview of offline and online decoding performance of finger movements

Table S5. Overview of results of functional tests

Movie S1. Single finger control of prosthetic hand

Movie S2. Functional outcomes: 4.5 DoF simultaneous and proportional control

# References


1. M. Ortiz-Catalan, Engineering and surgical advancements enable more cognitively integrated bionic arms. *Sci. Robot.* **6**, 4–6 (2021).

2. T. A. Kuiken, Targeted Muscle Reinnervation for Real-time Myoelectric Control of Multifunction Artificial Arms. *JAMA* **301**, 619 (2009).

3. L. A. Miller, R. D. Lipschutz, K. A. Stubblefield, B. A. Lock, H. Huang, T. W. Williams, R. F. Weir, T. A. Kuiken, Control of a Six Degree of Freedom Prosthetic Arm After Targeted Muscle Reinnervation Surgery. *Arch. Phys. Med. Rehabil.* **89**, 2057–2065 (2008).

4. M. G. Urbanchek, Z. Baghmanli, J. D. Moon, K. B. Sugg, N. B. Langhals, P. S. Cederna, Quantification of Regenerative Peripheral Nerve Interface Signal Transmission. *Plast. Reconstr. Surg.* **130**, 55–56 (2012).

5. M. G. Urbanchek, T. A. Kung, C. M. Frost, D. C. Martin, L. M. Larkin, A. Wollstein, P. S. Cederna, Development of a Regenerative Peripheral Nerve Interface for Control of a Neuroprosthetic Limb. *Biomed Res. Int.* **2016**, 1–8 (2016).

6. P. P. Vu, A. K. Vaskov, Z. T. Irwin, P. T. Henning, D. R. Lueders, A. T. Laidlaw, A. J. Davis, C. S. Nu, D. H. Gates, R. B. Gillespie, S. W. P. Kemp, T. A. Kung, C. A. Chestek, P. S. Cederna, A regenerative peripheral nerve interface allows real-time control of an artificial hand in upper limb amputees. *Sci. Transl. Med.* **12**, 1–12 (2020).

7. M. Ortiz-Catalan, B. Hakansson, R. Branemark, An osseointegrated human-machine gateway for long-term sensory feedback and motor control of artificial limbs. *Sci. Transl. Med.* **6**, 257re6-257re6 (2014).

8. E. Mastinu, F. Clemente, P. Sassu, O. Aszmann, R. Brånemark, B. Håkansson, M. Controzzi, C. Cipriani, M. Ortiz-Catalan, Grip control and motor coordination with implanted and surface electrodes while grasping with an osseointegrated prosthetic hand. *J. Neuroeng. Rehabil.* **16**, 49 (2019).

9. M. Ortiz-Catalan, E. Mastinu, P. Sassu, O. Aszmann, R. Brånemark, Self-Contained Neuromusculoskeletal Arm Prostheses. *N. Engl. J. Med.* **382**, 1732–1738 (2020).

10. M. Ortiz-Catalan, R. Brånemark, B. Håkansson, J. Delbeke, On the viability of implantable electrodes for the natural control of artificial limbs: Review and discussion. *Biomed. Eng. Online* **11**, 33 (2012).

11. M. Ortiz-Catalan, J. Marin-Millan, J. Delbeke, B. Håkansson, R. Brånemark, Effect on signal-to-noise ratio of splitting the continuous contacts of cuff electrodes into smaller recording areas. *J. Neuroeng. Rehabil.* **10**, 22 (2013).

12. M. Ortiz-Catalan, R. Brånemark, B. Håkansson, BioPatRec: A modular research platform for the control of artificial limbs based on pattern recognition algorithms. *Source Code Biol. Med.* **8**, 11 (2013).

13. L. M. Hermansson, A. G. Fisher, B. Bernspång, A. C. Eliasson, Assessmet of Capacity for Myoelectric Control: A new Rasch-built measure of prosthetic hand control. *J. Rehabil. Med.* **37**, 166–171 (2005).

14. A. Middleton, M. Ortiz-Catalan, Neuromusculoskeletal Arm Prostheses: Personal and Social Implications of Living With an Intimately Integrated Bionic Arm. *Front. Neurorobot.* **14**, 18 (2020).

15. E. Mastinu, R. Branemark, O. Aszmann, M. Ortiz-Catalan, in *2018 40th Annual*

655 *International Conference of the IEEE Engineering in Medicine and Biology Society (EMBC)*,
656 (IEEE, 2018), vol. 2018-July, pp. 5174–5177.

657 16. L. E. Osborn, C. W. Moran, M. S. Johannes, E. E. Sutton, J. M. Wormley, C. Dohopolski, M.
658 J. Nordstrom, J. A. Butkus, A. Chi, P. F. Pasquina, A. B. Cohen, B. A. Wester, M. S. Fifer, R. S.
659 Armiger, Extended home use of an advanced osseointegrated prosthetic arm improves
660 function, performance, and control efficiency. *J. Neural Eng.* **18**, 026020 (2021).

661 17. C. Cipriani, C. Antfolk, M. Controzzi, G. Lundborg, B. Rosen, M. C. Carrozza, F. Sebelius,
662 Online Myoelectric Control of a Dexterous Hand Prosthesis by Transradial Amputees. *IEEE*
663 *Trans. Neural Syst. Rehabil. Eng.* **19**, 260–270 (2011).

664 18. E. M. Janssen, H. L. Benz, J. H. Tsai, J. F. P. Bridges, Identifying and prioritizing concerns
665 associated with prosthetic devices for use in a benefit-risk assessment: a mixed-methods
666 approach. *Expert Rev. Med. Devices* **15**, 385–398 (2018).

667 19. M. Ortiz-Catalan, B. Hakansson, R. Branemark, Real-Time and Simultaneous Control of
668 Artificial Limbs Based on Pattern Recognition Algorithms. *IEEE Trans. Neural Syst. Rehabil.*
669 *Eng.* **22**, 756–764 (2014).

670 20. H. Y. N. Lindner, A. Langius-Eklöf, L. M. N. Hermansson, Test-retest reliability and rater
671 agreements of assessment of capacity for myoelectric control version 2.0. *J. Rehabil. Res.*
672 *Dev.* **51**, 635–644 (2014).

673 21. E. J. Earley, J. Zbinden, M. Munoz-Novoa, E. Mastinu, A. Smiles, M. Ortiz-Catalan,
674 Competitive motivation increased home use and improved prosthesis self-perception after
675 Cybathlon 2020 for neuromusculoskeletal prosthesis user. *J. Neuroeng. Rehabil.* **19**, 1–11
676 (2022).

677 22. D. Farina, I. Vujaklija, M. Sartori, T. Kapelner, F. Negro, N. Jiang, K. Bergmeister, A.
678 Andalib, J. Principe, O. C. Aszmann, Man/machine interface based on the discharge timings
679 of spinal motor neurons after targeted muscle reinnervation. *Nat. Biomed. Eng.* **1**, 0025
680 (2017).

681 23. S. Muceli, K. D. Bergmeister, K.-P. Hoffmann, M. Aman, I. Vukajlija, O. C. Aszmann, D.
682 Farina, Decoding motor neuron activity from epimysial thin-film electrode recordings
683 following targeted muscle reinnervation. *J. Neural Eng.* **16**, 016010 (2019).

684 24. J. A. George, T. S. Davis, M. R. Brinton, G. A. Clark, Intuitive neuromyoelectric control of
685 a dexterous bionic arm using a modified Kalman filter. *J. Neurosci. Methods* **330**, 108462
686 (2020).

687 25. B. Ahkami, E. Mastinu, E. Earley, M. Ortiz-Catalan, Extra-neural signals from severed
688 nerves enable intrinsic hand movements in transhumeral amputations. *Under Rev.* .

689 26. K. Hagberg, E. Häggström, M. Uden, R. Brånemark, Socket Versus Bone-Anchored Trans-
690 Femoral Prostheses. *Prosthetics Orthot. Int.* **29**, 153–163 (2005).

691 27. H. Van de Meent, M. T. Hopman, J. P. Frölke, Walking Ability and Quality of Life in
692 Subjects With Transfemoral Amputation: A Comparison of Osseointegration With Socket
693 Prostheses. *Arch. Phys. Med. Rehabil.* **94**, 2174–2178 (2013).

694 28. A. Thesleff, E. Haggstrom, R. Tranberg, R. Zugner, A. Palmquist, M. Ortiz-Catalan, Loads
695 at the Implant-Prosthesis Interface During Free and Aided Ambulation in Osseointegrated
696 Transfemoral Prostheses. *IEEE Trans. Med. Robot. Bionics* **2**, 497–505 (2020).

697 29. E. Mastinu, L. F. Engels, F. Clemente, M. Dione, P. Sassu, O. Aszmann, R. Brånemark, B.
698 Håkansson, M. Controzzi, J. Wessberg, C. Cipriani, M. Ortiz-Catalan, Neural feedback

699 strategies to improve grasping coordination in neuromusculoskeletal prostheses. *Sci. Rep.*
700 **10**, 11793 (2020).

701 30. E. Mastinu, P. Doguet, Y. Botquin, B. Hakansson, M. Ortiz-Catalan, Embedded System for
702 Prosthetic Control Using Implanted Neuromuscular Interfaces Accessed Via an
703 Osseointegrated Implant. *IEEE Trans. Biomed. Circuits Syst.* **11**, 867–877 (2017).

704 31. B. Hudgins, P. Parker, R. N. Scott, A new strategy for multifunction myoelectric control.
705 *IEEE Trans. Biomed. Eng.* **40**, 82–94 (1993).

706 32. C. M. Light, P. H. Chappell, P. J. Kyberd, Establishing a standardized clinical assessment
707 tool of pathologic and prosthetic hand function: Normative data, reliability, and validity.
708 *Arch. Phys. Med. Rehabil.* **83**, 776–783 (2002).

709 33. J. G. M. Burgerhof, E. Vasluian, P. U. Dijkstra, R. M. Bongers, C. K. van der Sluis, The
710 Southampton Hand Assessment Procedure revisited: A transparent linear scoring system,
711 applied to data of experienced prosthetic users. *J. Hand Ther.* **30**, 49–57 (2017).

712

## 713 Acknowledgements

714 The authors thank the subject who participated in this study and his family for their time and
715 efforts. The authors further thank David Martín Espinosa for preparing the schematic
716 illustration in Figure 1.

717

718

## Funding

Promobilia Foundation grant 19500 (MOC)

IngaBritt and Arne Lundbergs Foundation grant 2018-0026 (MOC)

Swedish Research Council (Vetenskapsrådet) grant 2020-04817 (MOC)


## Author Contributions

M.O.C., P.S., and R.B. conceived the surgical approach. M.O.C., E.M., and R.B. developed the technologies used in this study. P.S. and R.B. performed the surgeries. J.Z., E.M., E.E., and M.M.N conducted the experiments. J.Z. analyzed the data. J.Z. and M.O.C. drafted the manuscript. All authors revised and approved the final manuscript.

## Competing interests

J.Z., P.S., E.E., and M.M.N. declare no competing interests. E.M. and M.O.C. have consulted for Integrum AB. M.O.C. and R.B. hold shares of Integrum AB. M.O.C. and R.B. are co-inventors on patent # US9579222B2 entitled “Percutaneous gateway, a fixing system for a prosthesis, a fixture and connecting means for signal transmission “, which is held by Integrum AB.

## Data availability

All data needed to evaluate the conclusions in the paper are present in the paper and the Supplementary Materials.

# Figure captions

**Figure 1 Schematic illustration and X-ray of a highly integrated human-machine interface.**

**Figure 2 Electrical resistance of epimysial, intramuscular, and cuff electrodes over time.** (a) Resistance of the epimysial electrodes on unreconstructed and reinnervated native muscles (n=4). (b) Resistance of the intramuscular electrodes in unreconstructed muscles, reinnervated native muscles, and reinnervated free muscle grafts (n=8). (c) Resistance of the ring and three discrete contacts the cuff electrode around a fascicle of the median nerve (n=4).

**Figure 3 Representative examples of the raw EMG signals over time.** (a) Raw EMG signals for electrodes in an unreconstructed muscle, (b) a reinnervated native muscles, and (c) a free muscle graft. Each EMG recording consists of three seconds sequences of three active movement and rest periods.

**Figure 4 Signal to noise ratio development over time.** Change of signal to noise ratio of (a) four electrodes in unreconstructed muscles (n=1 movement), (b) three electrodes on/in reinnervated native muscles (n=6, n=3, and n=4 movements from left to right, respectively), and (c) five electrodes within reinnervated free muscle grafts (n=6, n=3, n=5, n=3, and n=3 movements, from left to right, respectively). The grey areas depict the standard deviation around the average values over the number of movements. For all signal to noise ratio calculations, only data of the main movements that anatomically corresponded to the electrode placement/innervation site were considered (see Methods for more details).

**Figure 5 Offline and online decoding performance.** Decoding performance using gross (hand open/close, supination/pronation, wrist flexion/extension, and elbow flexion/extension) and single finger movements over a two-year period. (a) Offline accuracy of nine gross movements (n = 9 movements, 100 repetitions). (b) Motion test completion rate for gross movements (n = 9 movements, 3 trials), where 100% indicates that all required movements were performed. (c) Completion time (time between the first decoded movement and twenty correct predictions of the promoted movement) and (d) accuracy (percentage of correct predictions) for the four degrees of freedom during the motion test. (e) Offline accuracy of individual fingers (n = 11 movements, 100 repetitions). (f) Completion rate, (g) completion time, and (h) accuracy for the motion test for individual finger decoding (n = 11 movements, 3 trials each).

**Figure 6 Results of functional tests.** (a) ACMC outcome, scored between 0 and 100, for a 1.5 DoF control scheme using surface electrodes before surgery and implanted electrodes at week 8 and 59 after surgery. A higher score indicates a higher capacity for myoelectric control. (b) ACMC outcome when using a 4.5 DoF simultaneous and proportional control scheme with the electro-neuromuscular constructs and without prior training. (c) Outcome of SHAP for surface electrodes before surgery and implanted electrodes at week 8 and 59 after surgery. The circles indicate the linear Index of Function, scored between 0 and 100, for each task of the SHAP (n = 26 tasks). The horizontal black line shows the weighted linear Index of Function (W-LIOF), where a higher score represents greater prosthetic functionality during activities of daily living. (d) Outcome of SHAP (n = 26 tasks) when using a 4.5 DoF simultaneous and proportional control scheme with the electro-neuromuscular constructs and without prior training.